Received: 21 July 2023 | Revised: 11 October 2023 | Accepted: 13 November 2023

DOI: 10.1002/cjce.25154

RESEARCH ARTICLE

THE CANADIAN JOURNAL OF CHEMICAL ENGINEERING

Kinetic growth model and metabolic effect of a bacterial consortia from a petrochemical processing plant

Alicia Prithiraj | **Shepherd Tichapondwa** | **Evans M. N. Chirwa**

Department of Chemical Engineering, University of Pretoria, Pretoria, South Africa

Correspondence
Alicia Prithiraj, Department of Chemical Engineering, University of Pretoria, Pretoria, South Africa.
Email: alicia.prithiraj@gmail.com

Funding information
National Research Foundation, Grant/Award Numbers: EQP180503325881, TTK18024324064; Rand Water Chair in Water Utilization

Abstract

This study focused on presenting the newly developed growth model for bacterial species present in a petrochemical processing plant in South Africa. The findings of the study serve as a theoretical basis for future experiments aimed at understanding the formation of bacterial metabolites as the bacteria develops. An unstructured kinetic model using AQUASIM 2.3, together with experimental spectrophotometric results, were used to evaluate the growth of Gram-negative bacteria in a batch reactor system. Spectrophotometer results showed the absence of a stationary phase. The exponential bacterial growth phase supported the total organic carbon (TOC) results, showing that bacterial growth occurred on days 6 and 13; this is rarely reported in literature, as the growth in this system was much slower than the growth of single-strain studies. The TOC concentration values indicated that carbon sources did not deplete in the death phase, suggesting the presence of a long-term stationary phase and the production of acetate. The presence of *Pseudomonas* sp. and sulphate-reducing bacteria (SRB) are commonly reported in industrial systems as they play a role in equipment failure in industry. However, in this multispecies study, methods using third generation sequencing together with high-performance liquid chromatography (HPLC) have shown that the selective attachment and production of acetate by abundant *Clostridium* sp. has ascertained their role in equipment failures in the petrochemical environment.

KEYWORDS

kinetic model, metabolites, mixed bacterial culture, petrochemical industry

1 | INTRODUCTION

Bacteria in wastewater treatment processes play an important role in the depletion of nutrient carbon source (substrate concentration). The substrate can also be comprised of domestic and industrial waste.[1,2] When the bacteria degrade the nutrient, they continuously grow until the concentration of the nutrient is completely depleted.[2] The same concept applies in petrochemical cooling water systems, where hydrocarbons (substrate) such as jet fuels, petrol, and diesel are utilized by bacteria to grow and survive. Cooling towers provide a stable

environment for microbial growth owing to the temperature, pH, continuous aeration, nutrients, and sunlight, resulting in diverse microbial populations.[3] A study by Tsao et al.[4] investigated the microbial diversity of three cooling tower basins over the course of one year and found that bacterial diversity in all three cooling towers was broadly comparable to other freshwater systems such as *Sphingomonadales*, *Psuedomonadales*, *Rhizobiales*, and *Burkholderiales*. Although each cooling tower showed a dynamic site-specific microbial community, the shared taxa on the three locations mainly included groups generally associated with slime-forming bacteria such as *Pseudomonadales* and *Firmicutes*. Bacterial growth is typically described in four phases[5]; however, most authors do not make mention of the long-term stationary phase.[6] In this study, the four phases were evaluated together with the fifth phase called the long-term stationary phase. The lag phase is observed as a delay before exponential growth, the exponential phase is where cell division continues at a constant rate, the stationary phase is usually seen when the conditions become unfavourable for growth and bacteria stop replicating,[7–9] the death phase is seen as the phase where cells lose viability, and finally, the long-term stationary phase occurs, which can continue for years.[6] Bacterial metabolites play an important role in industrial equipment failures. A study by Zhu et al.[10] highlighted that the culture plate method is not effective in revealing the complexities that exist during multispecies bacterial attachment to industrial grade steel surfaces. The study also detected an abundance of *Clostridium* sp. which was not commonly reported in the petrochemical industries and may play a key role in industry equipment failures.[10] It has been postulated that various species present in a mixed bacterial culture may inhibit each other, leading to the production of organic acids which may impact the life-time of industry equipment.[11] A maritime study by Wang et al.[12] investigated the corrosive properties of the single-strain *Bacillus subtilis*; although the bacteria had developed biofilm which initiated localized corrosion, corrosion was then aggravated by the acidity of the bacterial metabolite.

Microbial growth kinetics have been the subject of many scientific studies and have many consequences for our society.[13] A combination of mathematical modelling and experimental data give a meaningful and quantitative interpretation of the experimental results that reveal new aspects of microbiology physiology.[13] A Monod model was presented in this study which highlighted that maximum specific growth rate is unique for every bacterial culture.[14]

In light of the above fact, this multispecies study used culture characterization methods on industry grade steel together with HPLC to give insight on the key players responsible for equipment failures in the petrochemical industry.

2 | MATERIALS AND METHODS

2.1 | Bacteria, media, and culture conditions

A perforated (0.178 mm) stainless steel mesh, designed to collect bacteria, was inserted in the cooling tower coupon rack, where cooling water was supplied at a temperature of 35°C at low flow. After 11 months, the mesh was removed from the coupon rack using sterilized tweezers and inserted in a sterile sample bag containing cooling tower water. The mesh was then inserted in a 1 L glass batch reactor with a screw-on lid containing media which was prepared using 0.5 g KH_2PO_4, 1 g NH_4Cl, 4.5 g Na_2SO_4, 0.005 g $CaCl_2 \cdot 2H_2O$, 0.06 g $MgSO_4 \cdot 7H_2O$, 12 g 50% solution sodium lactate, 1 g yeast extract, 0.004 g $FeSO_4 \cdot 7H_2O$, and 5 g $Na_3C_6H_5O_7$ sodium citrate mixed in 1 L distilled water. The batch reactor was incubated at a constant temperature of 35°C at aerobic conditions, similar to the cooling tower conditions. The initial pH of 6.52 was adjusted to 7 using 5 M NaOH. Tryptone soya agar (TSA) plates media was prepared using 40 g of TSA in 1 L distilled water. MTT solution was prepared in a dark room using 5 mg of 3-(4,5-dimethylthiazol-2-yl)-2,5-diphenyl tetrazolium (MTT) powder in 1 mL distilled water filtered into a 2 mL vial and frozen at −72°C. Media, distilled water, and instruments used were autoclaved at 121°C at a pressure of 1.5 kPa for 20 min. Similar industry batch media was prepared by Prithiraj et al.[15] and Zhao et al.[16]

2.2 | Metabolic activity

Metabolic activity was evaluated in a batch reactor containing prepared media inoculated with a mixed bacterial culture as described in Section 2.1. The batch media was gently mixed from side to side before duplicate 2 mL aliquots of sample were extracted. One sample was filtered and the other was not filtered. Vials were diluted with 3 mL of autoclaved distilled water. The diluted samples including 0.2 mL MTT solution was added to 2 mL vials. The 2 mL vials were placed in an incubator at 35°C for 60 min. Dimethyl sulphoxide (DMSO) was added before measuring absorbance using a Hatch DR 6000 spectrophotometer. Metabolic activity was calculated using the unfiltered sample absorbance value subtracted by the filtered sample absorbance value. Measurements were conducted in duplicates. Figure 1 summarizes the process followed.

2.3 | Monod model

The Monod model was first introduced by Jacques Monod in 1942 to describe the relationship between

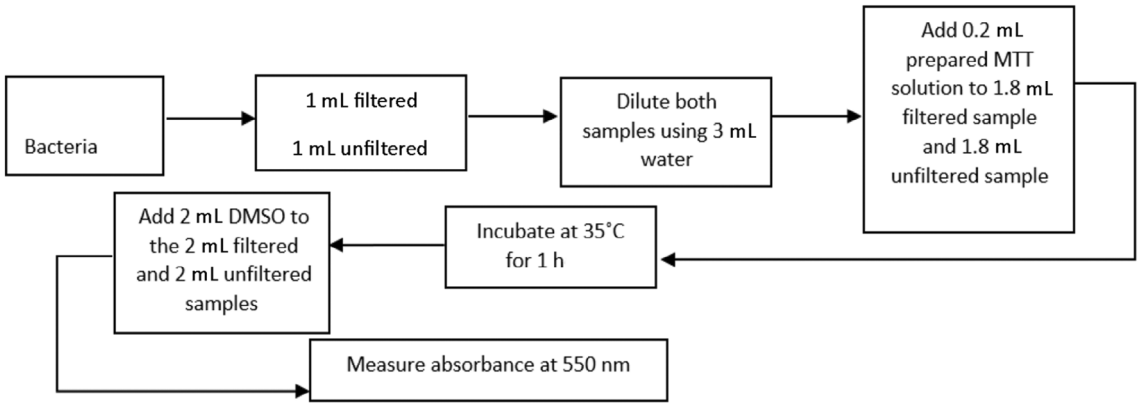

FIGURE 1 Process flow diagram to measure absorbance. DMSO, dimethyl sulphoxide; MTT, 3-(4,5-dimethylthiazol-2-yl)-2,5-diphenyl tetrazolium.

specific growth rate and substrate utilization rate in a bioreactor.[14] The model can be defined in two forms: based on substrate concentration only, and on both substrate and biomass concentration. For bacterial growth, Monod formulated an equation which is presented as Equation (1).

$$\mu = (\mu_{\max} S)/(K_s + S), \tag{1}$$

where S is the concentration of the nutrient in the media at time t and μ is the specific growth rate. It should be noted that μ does not start at zero due to the degradation of substrate by bacteria for maintenance energy. $\mu_{\max}$ is the maximum specific growth rate, and this value cannot be negative as it is the maximum value for growth rate. K_s (constant) = half-life saturation constant when $\mu = \mu_{\max}/2$; $S = K_s$.

2.4 | Total organic carbon (TOC) and high-performance liquid chromatography (HPLC)

The total carbon in the bacterial media was measured using a Teledyne (Tekmar 14-9600-200, United States) TOC analyzer. Samples were filtered using 0.45 µm syringe filter under sterile conditions, then diluted by a factor of 1000. The machine uses a voltage of 230 and 2.50 amp; the machine conforms to UL STD 61010A-1 certified to CSA Standard C22.2 N0.1010.1.

HPLC analysis was conducted to evaluate the degradation of the specific carbon sources (lactic acid and citric acid) in the batch reactor over time. A high-performance liquid chromatographic system equipped with a UV/Vis detector and a BioRad Aminex (HPX-87, United States) column was used. The detector was set at 210 nm. The flow rate of the 0.5 mM sulphuric acid mobile phase was set at 10 µL/min, using 10 µL injection volume if the samples and the column temperature were set at 35°C.

Simulated concentration models for depletion of lactate and citrate and sensitivity models were generated using AQUASIM 2.3 software. Experimental measurements from the HPLC analysis were included in the model using first order batch reactor kinetics.

2.5 | Colony forming units (CFU)

The number of live heterotrophic bacteria was measured using the standard plate count method.

Bacteria plating was carried out under a laminar flow hood. All instruments were autoclaved before use. The plates were wrapped in parafilm and placed in a fridge at −3°C. Colony forming units were calculated using Equation (2).

$$\frac{\log \text{CFU}}{\text{ML}} = \log(N \times F), \tag{2}$$

where N is the plate count (number of colonies counted on the plate), F is the dilution factor, and ML is the volume of culture plate.

2.6 | 16S rDNA gene sequencing on colony plates

TSA spread plates for days 3, 6, 9, and 13 were analyzed using 16S rDNA gene sequencing.

The strain identification was based on the plus/minus 600 bp partial sequence of the 16S rDNA gene of the organisms using a Veriti 96 Well Thermal Cycler (AB Applied Biosystems). The sequences were compared against the GenBank of the National Centre for

Biotechnology in the United States of America using a basic BLAST search.

The 16S gene profiling was started by purifying all polymerase chain reaction (PCR) products by adding 2 U/μL of Exonuclease 1 (Thermo Scientific) and 2 U/μL of FastAP (Thermo Scientific). This was followed by incubation on the T100TM Thermal Cycler (BioRad) at 37°C for 15 min to activate the enzymes and a second incubation at 85°C for 15 min. Sometimes, a second amplification product remained after cleaning; therefore, a Zymoclean Gel DNA Recovery Kit (Zymo Research) was used to purify the band of the expected size.

The purified products were then sequenced using the BigDye Terminator v3.1 Cycle Sequencing kit (Thermo Fisher Scientific, USA). The AB13100 Automated Capillary DNA sequencer (Thermo Fisher Scientific, Carlsbad, USA), was used to determine DNA sequence chromatograms from the purified sequencing products.

A separate batch reactor with the same prepared media and culture collection method as discussed in Section 2.1 now included a carbon steel coupon that was used to conduct 16S rDNA gene sequencing on a smooth finished coupon by swabbing the coupon using a sterile swab. Genomic DNA (gDNA) extraction (Zymo Research) was conducted on the swabs. The extracted gDNA was amplified in a PCR machine (Eppendorf Master cycler Nexus Gradient). The 27F and 1492R universal primer pair was used.[16] This was done in order to target the V1 and V9 region of the bacterial 16S rDNA gene. The amplicons were barcoded with Pacbio M13 barcodes for multiplexing through limited PCR. The resulting barcoded amplicons were quantified and a pooled equimolar and AMPure PB bead-based purification step was then performed. The PacBio SMRTbell library was prepared from the pooled amplicons following the manufacturer's protocol. Sequencing primer annealing and polymerase binding was done following the SMRTlink software protocol to prepare the library for sequencing on the PacBio Sequel IIe system.

Samples were sequenced on the Sequel system by PacBio software. Raw subreads were processed through the SMRTlink (v9.0) software and USEARCH. The taxonomic information was determined based on the Ribosomal database project's 16s database v16. The taxa classification percentage abundance reports were created using inhouse Python script. Highly accurate reads were processed via circular consensus sequences (CCS) and VSEARCH software.

2.7 | Alloy preparation

The carbon steel coupon, measuring 1 cm by 1 cm, was polished to 3 micron using silicon carbide waterproof paper and 3-micron polish. The coupons were polished using a Struers (Tegramin – 30, United States, Cleveland) automatic polishing machine for 3 min, using a force of 35 N at 300 revolutions per minute. Under a laminar flow hood, carbon steel alloys were fastened on cable ties and sterilized for 1 h using 70% ethanol. The fastened coupons were inserted into the batch reactor containing the media inoculated with a mixed bacterial culture. Coupons were rinsed three times to remove loosely attached bacteria.

3 | DISCUSSION

3.1 | Metabolic activity

Figure 2 presents the different phases of growth on multi-species bacteria collected from a cooling tower in a petrochemical proccessing plant. The lag phase was observed from days 1–6. In comparison to the single-species studies conducted by Kuang et al.[17] and Wang et al.,[12] where the lag phase is usually observed from days 1–2, the bacterial consortia in the current study showed a much slower growth rate. The lag phase is generally poorly understood, primarily because of a lack of data that describe the underlying physiological and molecular processes.[18] It has been assumed that the lag phase allows acclimation of the bacterial cells and exploration of the new environment.[8] There was no stationary phase observed; this was possibly due to a high substrate utilization rate by the bacteria, resulting in quicker growth and death phase. This hypothesis is guided

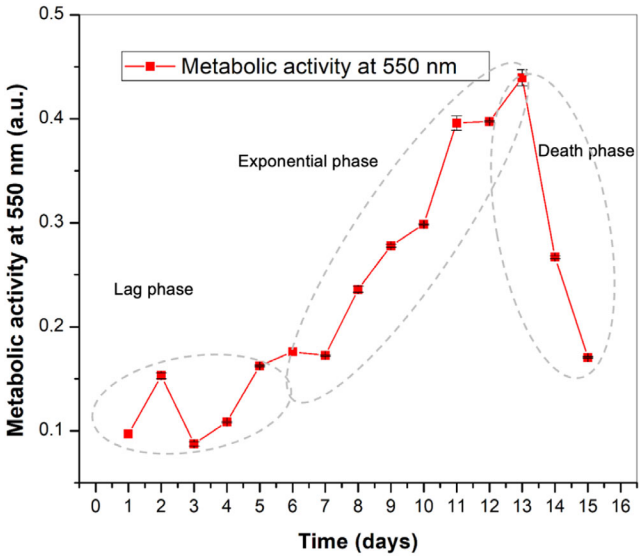

FIGURE 2 Bacterial growth curve (metabolic activity at 550 nm). Growth phases are indicated with a grey dotted line, media was incubated at 35°C, and aerobic conditions exist.

by the fact that the bacteria originate from a petrochemical environment which tends to have sufficient concentrations of hydrocarbons as their food source in continuous supply and utilized the limited carbon sources at a high rate.[19] For future investigations, it would be worthwhile to evaluate the bacterial growth phases using hydrocarbons that are introduced into the cooling tower systems such as diesel and jet fuel (Table 1). Table 1 presents the composition and hydrocarbon content in the cooling water. The composition of the cooling water will always vary due to operational demands; therefore, it was impossible to prepare a batch media to the exact composition as the cooling water. The peak in growth was reached on day 13, where Gram-negative bacteria then entered the death phase the day after. This is seen as an uncommon phenomenon, as the peak in growth was previously reported to be shortly after day 2.[12,17] In the death phase, the Gram-negative bacteria started to lose viability; however, there were viable Gram-positive bacteria which could not be quantified using the spectrophotometer and will be discussed in the sections below.

3.2 | Kinetic growth model using Monod equation

The growth characteristics typically found in batch flask systems are shown in Figure 3. This is also the type of growth that would be expected under conditions in a natural environment where substrate and nutrients are limited.[5] According to Contois,[20] the use of simple substrates, such as lactate used in this study, and homogenous cultures produce a more accurate Monod model. It is to be noted that the Monod model does not account for the lag, death, or long-term stationary phases.[21]

In the present model, it was observed that there was a fairly fast and sharp decrease in the substrate concentration, with most of it being consumed within the first day of the growth process. This was accompanied by a gradual increase in the specific growth rate with a maximum rate of 0.45 1/day observed on day 13. The specific growth rate at this point is independent of the substrate concentration; this means that if the substrate concentration were to be increased in this system, there would be no

pH	Zn[a]	Mg[a]	Ca[a]	Na[a]	Fe[a]	NH_3[a]	P[a]	M-Alk[a]	Silica[a]	TOC[a]
8.59	0.53	24.12	34.28	32.34	0.17	0.10	0.00	156	4.38	10.26
8.68	0.53	29.46	49.68	43.10	0.23	1.33	0.22	173	6.37	10.28
6.72	0.43	21.59	29.09	35.61	0.08	0.56	0.00	133	5.15	10.84
8.09	0.92	30.68	45.02	46.92	0.29	0.05	0.00	144	8.38	7.72
7.70	0.70	30.52	39.04	37.40	0.19	0.35	0.12	156	4.09	8.38

Abbreviations: M-Alk, the amount of carbonate in the water down to a pH of 4.6; TOC, total organic carbon.
[a]Values are presented in mg/L.

TABLE 1 Cooling water composition.

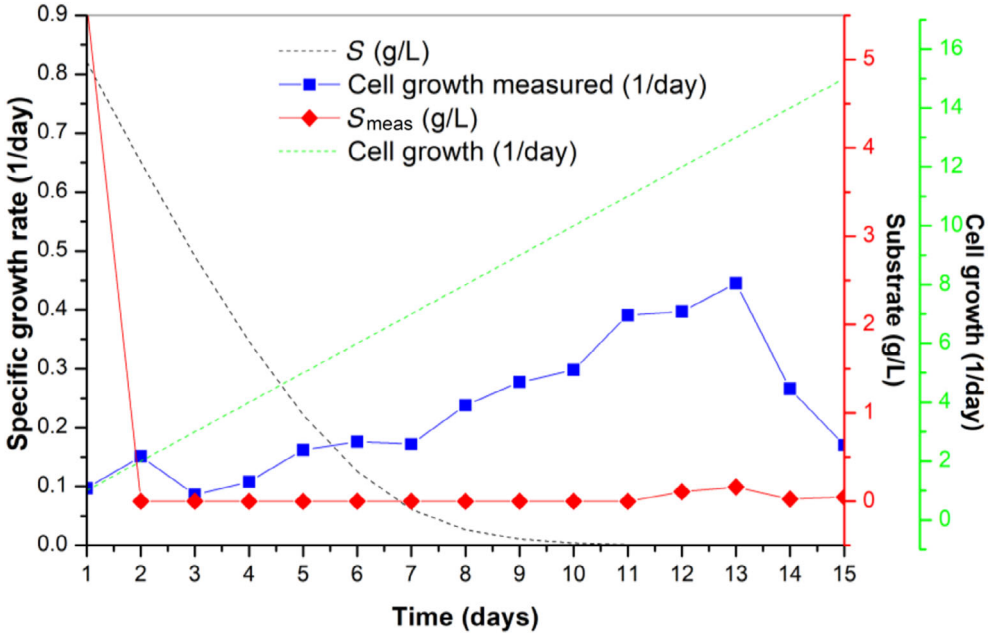

FIGURE 3 Monod model with lactate as the substrate. The green and black lines indicate the simulated curves, and the blue and red lines indicate the measured values.

further effect on the specific growth rate. The current model supports this statement, where an increase in lactate concentration was observed on days 12–15. In the present model, the lag, exponential, and death phases were seen, with the absence of the stationary and long-term stationary phases. In the simulated curve, only the exponential phase of growth was observed, where the maximum specific growth rate was reached much faster with a value of 0.22 1/day on Day 5. Overall, the Gram-negative species in this system performed better under low substrate conditions compared to the simulated model, especially during starved conditions (0 g/L). From the model, specific growth rate (μ) can be determined at different phases of the growth curve, which gives insight about the microorganisms in the system.

3.3 | Colony forming units

The CFU graph in Figure 4 presents data on the TSA plates from day 3 (lag phase). The number of bacteria in the TSA plates peaked on days 7 and 9, with the highest peak observed on day 13. These days are supported by the growth curve (Figure 2). However, the CFU results showed that there was still bacterial growth on day 15; this may be due to Gram-positive bacteria that could not be measured using the spectrophotometer.

3.4 | 16S rDNA gene sequencing

16S rDNA sequence on colony plates revealed that the dominant bacterial strain was the Gram-negative *Pseudomonas aeruginosa* motile bacterium on days 3, 6, and 13 (Table 2).[22] This aerobic slime-forming bacterium is commonly associated with marine and industry equipment failures.[23,24]

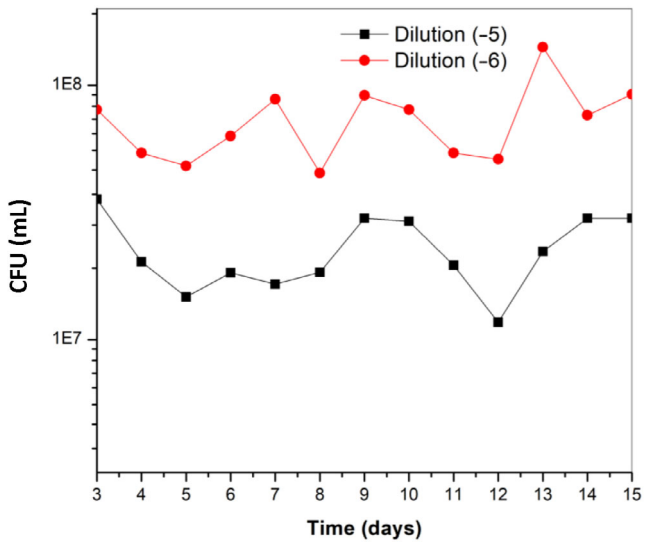

FIGURE 4 Colony forming units (CFU) from day 3 to day 15 at 35°C.

It has been reported that *Pseudomonas* sp. can initiate and accelerate the corrosion process.[23,25] 16S rDNA did not detect sulphate-reducing bacteria (SRB) usually associated with corrosion.[26] It was seen in the surface attachment studies that the dominant and abundant lactic acid bacterium (LAB) was *Clostridium* sp. (Figure 5), which are capable of producing organic acids.[27] The impact of the bacterium on corrosion was limited in this study.

3.5 | Substrate analysis

In Figure 6, the lactate and citrate that were added to the system fully depleted after day 1; however, carbon content was observed during the 15 days, suggesting that bacteria produced carbon sources (lactate and acetate) to adapt and survive in order to grow.[9]

3.5.1 | Carbon sources

It was seen from the data in Figure 6 that bacteria started producing lactic acid from day 12 (0.09 g/L). Other organic acids are also produced from the bacteria, such as acetic acid.[28] Acetic acid was discovered at later growth stages. Due to the detection of acetate and elevated TOC values from day 1 despite the rapid depletion of both lactic acid and citric acid, it is hypothesized that acetate may be produced from the early stages of bacterial growth, and that the samples must be left for a longer period in the HPLC to ascertain the presence of acetic acid at early stages. Acetic acid is considered to be one of the most common low carbon chain fatty acids and is highly corrosive to carbon steel.[12] Acetate is known to be produced by the homofermentative conversion of glucose by *Clostridium* bacteria identified as 'acetogenic'.[28] The TOC results revealed that carbon sources were gradually depleting from days 1–5, and a slight increase in carbon content was seen on day 6. The carbon content decreased from days 7 and 8, and a sudden increase of 3.1 g/L was seen on day 9. The carbon source gradually decreased again until day 13 where a sudden spike was noticed of 2.1 g/L, which closely resembled the concentration of acetate. Thereafter, a gradual decline in carbon source was seen; the carbon value then increased to about 0.71 g/L after day 14. The findings are supported by the growth curve graph (Figure 2), where spikes in carbon values are seen in the exponential phase of bacterial growth. However, after

TABLE 2 16S rDNA gene sequencing results on selected colony plates highlighting the dominant bacteria.

	Isolate	Result	% sequence identity	Gram-negative or Gram-positive
1	3S1 (Day 3/SRB) Brown	*Pseudomonas aeruginosa*	99.7	Gram-negative
2	3 T1 (Day 3/TSA)	*Plesiomonas shigelloides*	99.3	Gram-negative
3	3 T2 (Day 3/TSA)	*Enterococcus faecalis*	99.9	Gram-positive
4	3 T3 (Day 3/TSA)	*Bacillus thuringiensis*	100	Gram-positive
5	6 T1 (Day 6/TSA)	*Acinetobacter junii*	100	Gram-negative
6	6 T2 (Day 6/TSA)	*Shewanella xiamenensis*	99.3	Gram-negative
7	6 T3 (Day 6/TSA)	*Morganella morganii*	98.6	Gram-negative
8	6 T4 (Day 6/TSA)	*Bacillus wiedmannii*	99.7	Gram-positive
9	6 T5 (Day 6/TSA) Black	*P. aeruginosa*	100	Gram-negative
10	13 T1 (Day 13/TSA)	*Acinetobacter guillouiae*	99.0	Gram-negative
11	13 T2 (Day 13/TSA)	*Bacillus thuringiensis*	99.8	Gram-positive
12	13 T3 (Day 13/TSA)	*P. aeruginosa*	100	Gram-negative

Abbreviations: SRB, sulphate-reducing bacteria; TSA, tryptone soya agar.

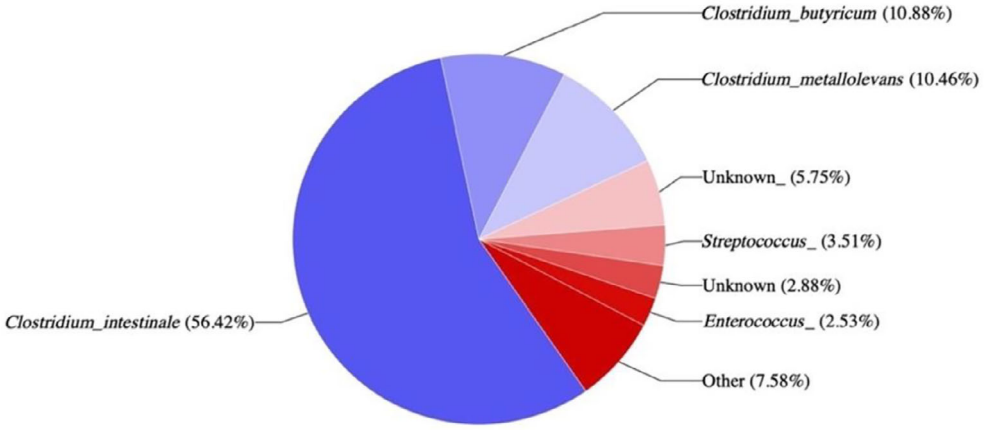

FIGURE 5 16S gene sequencing result of bacteria attached to smooth surface on day 3, indicating *Clostridium* sp. bacteria dominated the smooth surface and was not detected on colony plates.

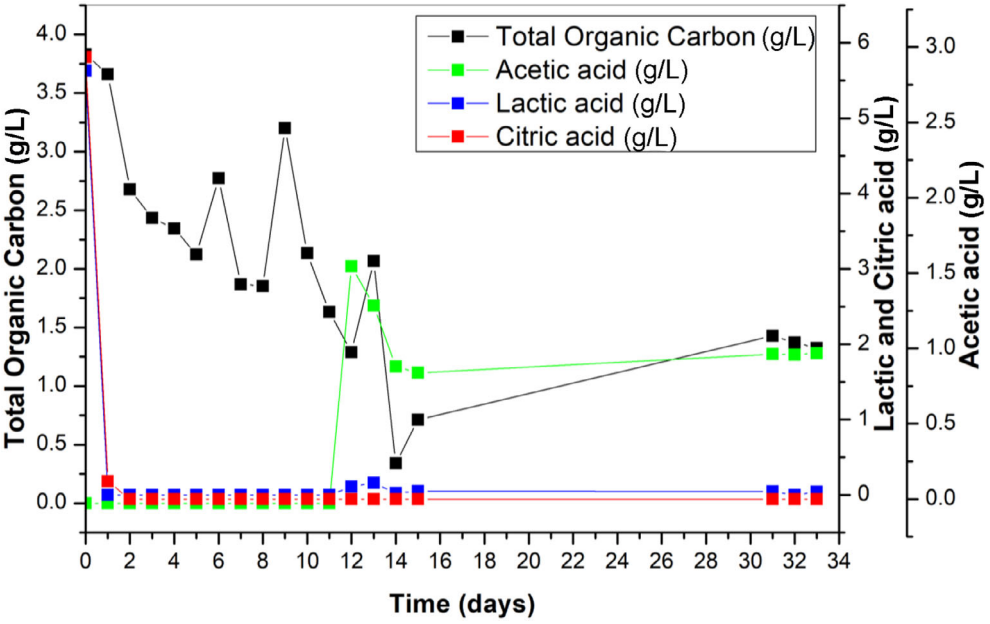

FIGURE 6 Carbon sources and total organic carbon (TOC) content. The media was incubated at 35°C in aerobic conditions.

day 14, bacterial activity was still evident due to production of carbon as seen in Figures 4 and 6. However, a decline in bacterial activity was seen in the growth curve after day 13 (Figure 2). The media was left for 15 more days, and TOC was evaluated on days 31–33. It was evident that there was still a significant amount of carbon content in the media at 1.43 g/L and no decrease, which further supports that the long-term stationary phase of bacterial growth exists and suggests the involvement of mainly Gram-positive bacteria. During prolonged starvation, certain bacterial species enter a continuous cycle of growth and death until there is renewal of favourable growth conditions; this means that Gram-positive bacterial species produce dormant spores in nutrient depleted conditions and the Gram-negative bacteria tend to acquire resistance.[9] This long-term stationary phase can be further investigated, as the number of days in this investigation was limited to 15. The sporadic TOC pattern observed in Figure 6 was due to bacteria utilizing and producing the carbon source to grow.

The presence of the organic acid known as acetate is directly related to the abundant *Clostridium* sp. that selectively attached to the industry grade steel surface (Figure 5). Moreover, the position put forward by Zhu et al.[10] was supported, as this study had shown that *Clostridium* sp. (Figure 5) was capable of producing organic acids involved in corrosion of steel; furthermore, the bacterium does not depend on carbon sources for long-term survival (Figure 6). Possible carbon sources to be further investigated will be discussed in the sections that follow.

3.6 | Kinetic models for lactic and citric acid degradation

Concentration degradation models (Figures 7 and 8) were done using AQUASIM 2.3 software, where the measured concentration is indicated by the black trend line. The error was within range as indicated by the blue dotted line. Carbon sources were depleted over the 15 days.

A general observation was that citric acid was utilized by bacteria at a lower rate than lactic acid.

3.6.1 | Lactate and acetate

Lactate and acetate are both required for bacterial growth of *Clostridium butyricum*.[27] Research adapted from bacteria utilizing lactate was chosen to present a possible metabolic pathway most likely identified for this system (Figure 9). These include lactic acid and acetic acid transformation to possible butyrate and other products by *C. butyricum*. Butyrate production as a metabolite will be further investigated in future studies, as it was not investigated in this study. LAB perform an important function as competitors and hydrogen producers which assist in the balance of bacterial diversity in bioreactors.[27,29]

3.6.2 | Citrate

Citrate is also known to influence the growth and metabolism of acetate. Earlier literature reported that heterofermentative

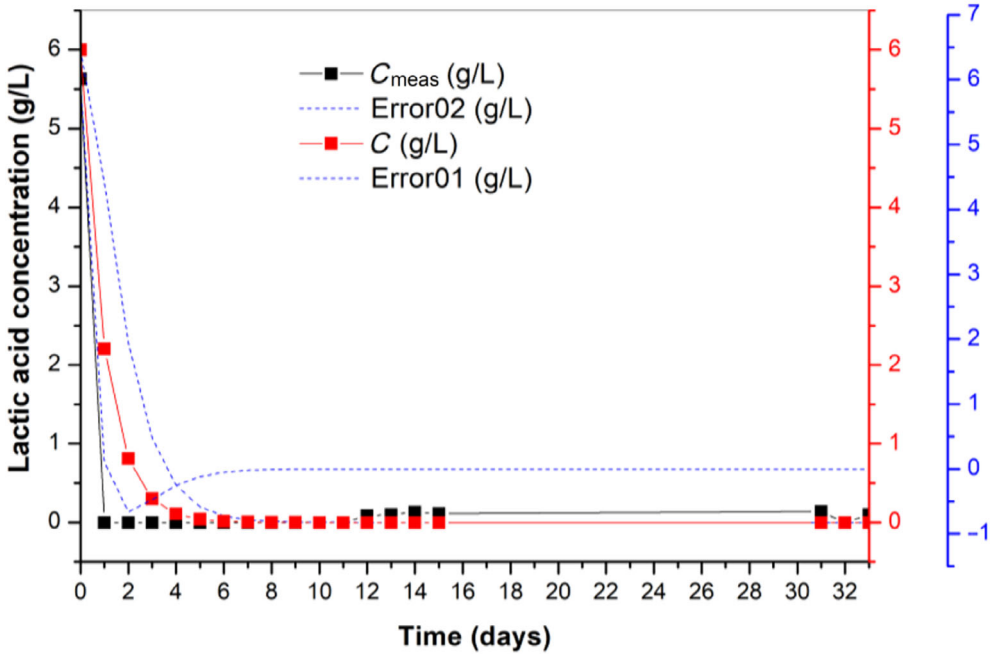

FIGURE 7 AQUASIM sensitivity model of the degradation of lactic acid concentration; experimental results are shown by the black curve.

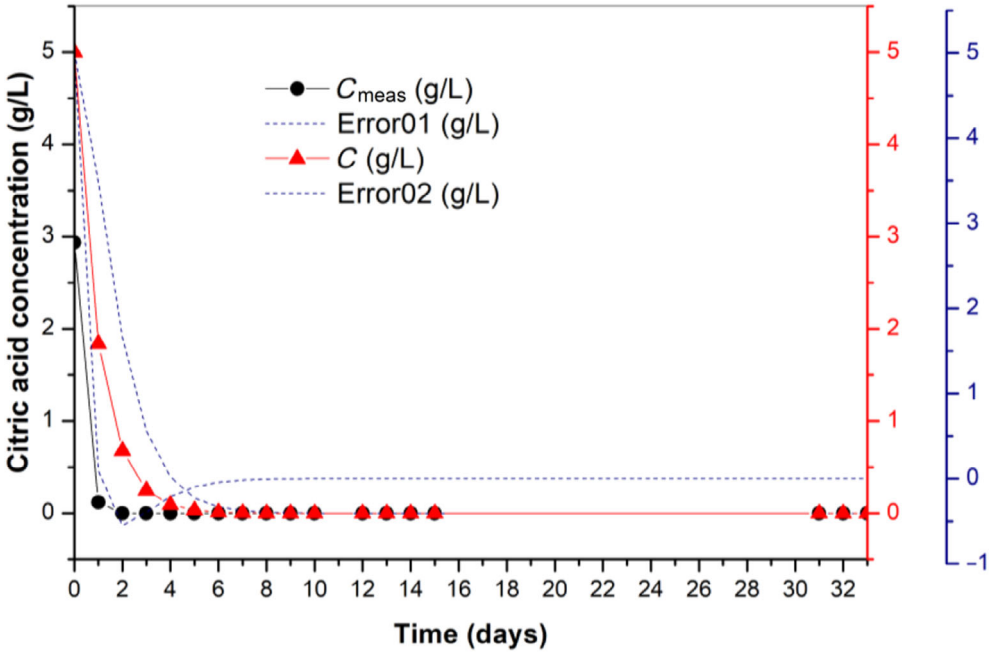

FIGURE 8 AQUASIM sensitivity model of the degradation of citric acid concentration; experimental results are shown by the black curve.

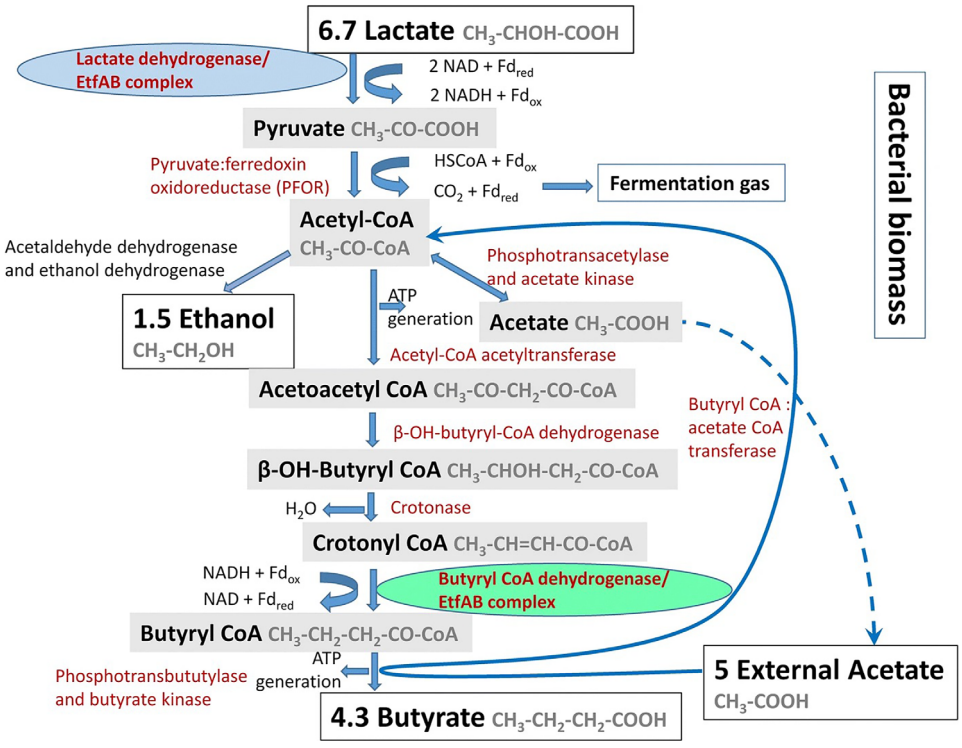

FIGURE 9 Metabolic pathway presented by Detman et al.[27] showing initial concentration of lactate being depleted by *C. butyricum* (dehydrogenase process) to form acetic acid and be converted to butyrate. The model does not account for utilization of citric acid, production of lactate, and possible acetoin as metabolites.

and homofermentative bacteria utilize citrate to produce acetylmethylcarbinol (acetoin)[29]; this metabolite was not evaluated in this study.

The metabolic by-products of a variety of bacterial species found in nature can support the growth of another while the attachment of another species could provide ligands allowing attachment of others. Competition for substrate and waste may be generated by the initial colonizers, which limits the diversity of the bacterial species.[30,31]

4 | CONCLUSIONS

The experimental growth curve showed no stationary phase; therefore, no prediction can be made on the bacterial growth of a mixed culture system. The long-term stationary phase is supported by TOC, CFU, and HPLC results, and further studies on the growth of Gram-positive bacteria in this system could be worthwhile. Growth of the bacteria in hydrocarbon batch systems will be carried out as future work. The spikes in

TOC values were seen in the exponential phase of the bacterial growth curve. Acetic acid and lactic acid were produced by Gram-positive bacteria from day 12 and were also seen on days 31–33. Metabolites such as butyrate and acetoin, with their corrosion related properties, can be investigated further. A general finding was that citric acid was utilized at a lower rate than lactic acid. Organic acids produced by the bacteria are associated with the mechanism of corrosion. However, the influence of bacterial organic acids on steel corrosion will be carried out in future work.

NOMENCLATURE

Symbols

C	simulated concentration of lactate and citrate (g/L)
C_{meas}	measured concentration of lactate and acetate (g/L)
S	concentration of the nutrient (g/L)

Greek letters

μ	specific growth rate (1/day)

Subscripts

s	half-life saturation
max	maximum
meas	measured

Dimensionless numbers

K_s	half-life saturation constant
N	number of colonies counted on the plate
F	dilution factor

AUTHOR CONTRIBUTIONS

Alicia Prithiraj: Conceptualization; methodology; formal analysis; writing – original draft; writing – review and editing; investigation. **Shepherd Tichapondwa:** Resources; writing – review and editing; funding acquisition; supervision. **Evans M. N. Chirwa:** Supervision; funding acquisition; writing – review and editing; resources; project administration.

ACKNOWLEDGEMENTS

The authors would like to thank the National Research Fund (NRF) of South Africa (Grant numbers: EQP180503325881, TTK18024324064) and the Rand Water Chair in Water Utilization awarded to Prof. Evans M. N. Chirwa and Prof. Shepherd Tichapondwa.

DATA AVAILABILITY STATEMENT

The data that support the findings of this study are available on request from the corresponding author. The data are not publicly available due to privacy or ethical restrictions.

ORCID

Alicia Prithiraj https://orcid.org/0000-0002-5129-9781

REFERENCES

[1] Y. Y. Choi, S. R. Baek, J. I. Kim, J. W. Choi, J. Hur, T. U. Lee, C. J. Park, B. J. Lee, *Water* **2017**, *9*, 409.
[2] M. Muloiwa, S. Nyende-Byakika, M. Dinka, S. Afr, *J. Chem. Eng.* **2020**, *33*, 141.
[3] M. Ludensky, in *Directory of Microbiocides for the Protection of Materials* (Ed: W. Paulus), Springer, Dordrecht **2004**.
[4] H. F. Tsao, U. Scheikl, C. Herbold, A. Indra, J. Walochnik, M. Horn, *Water Res.* **2019**, *159*, 464.
[5] R. M. Maier, I. L. Pepper, in *Environmental Microbiology*, 3rd ed. (Eds: I. L. Pepper, C. P. Gerba, T, J. Gentry), Academic Press, Oxford, UK **2015**, p. 37.
[6] S. E. Finkel, *Nat. Rev. Microbiol* **2006**, *4*, 113.
[7] B. M. Lund, T. C. Baird-Parker, G. W. Gould, *The Microbiological Safety and Quality of Food*, 1st ed., Aspen Publishers, Gaithersburg, MD **2000**, p. 342.
[8] M. T. Madigan, J. M. Martinko, J. Parker, *Brock Biology of Microorganisms*, 6th ed., Prentice-Hall, Upper Saddle River, NJ **2000**, p. 135.
[9] J. M. Navarro Llorens, A. Tormo, E. Martínez-García, *FEMS Microbiol. Rev.* **2010**, *34*, 476.
[10] X. Y. Zhu, J. Lubeck, J. J. Kilbane, *Appl. Environ. Microbiol.* **2003**, *69*, 5354.
[11] F. Leroy, L. De Vuyst, *Appl. Environ. Microbiol.* **2001**, *67*, 4407.
[12] Y. S. Wang, L. Liu, Q. Fu, J. Sun, Z. Y. An, R. Ding, Y. Li, X. D. Zhao, *Sci. Rep.* **2020**, *10*, 1.
[13] D. J. Mahanta, M. Borah, P. Saikia, *American International Journal of Research in Sciences, Technology, Engineering and Mathematics* **2014**, *8*, 2328.
[14] J. Monod, *Annu. Rev. Microbiol.* **1949**, *3*, 371.
[15] A. Prithiraj, I. O. Otunniyi, P. Osifo, J. van Der Merwe, *Eng. Failure Anal.* **2019**, *104*, 977.
[16] M. Zhao, C. Tyson, H. C. Chen, S. Paudel, R. Gitaitis, B. Kvitko, B. Dutta, *Syst. Appl. Microbiol.* **2022**, *45*, 126278.
[17] F. Kuang, J. Y. A. N. L. Wang, D. Zhang, *Electrochim. Acta* **2007**, *52*, 6084.
[18] M. D. Rolfe, C. J. Rice, S. Lucchini, C. Pin, A. Thompson, A. D. Cameron, M. Alston, M. F. Stringer, R. P. Betts, J. Baranyi, M. W. Peck, *J. Bacteriol.* **2012**, *194*, 686.
[19] A. Rajasekar, S. Maruthamuthu, N. Muthukumar, S. Mohanan, P. Subramanian, N. Palaniswamy, *Corros. Sci.* **2005**, *47*, 257.
[20] D. E. Contois, *Microbiology* **1959**, *21*, 40.
[21] J. D. Kong, *PhD Thesis*, University of Alberta (116 St & 85, Edmonton) **2017**.
[22] H. Li, E. Zhou, D. Zhang, D. Xu, J. Xia, C. Yang, H. Feng, Z. Jiang, X. Li, T. Gu, K. Yang, *Sci. Rep.* **2016**, *6*, 1.
[23] B. J. Little, J. S. Lee, R. I. Ray, *Electrochim. Acta* **2008**, *54*, 2.
[24] C. H. Liang, H. Wang, N. B. Huang, *J. Iron Steel Res* **2014**, *21*, 444.
[25] S. Shokrollahzadeh, F. Azizmohseni, F. Golmohammad, H. Shokouhi, F. Khademhaghighat, *Bioresour. Technol.* **2008**, *99*, 6127.
[26] H. Chen, Ö. Kimyon, H. L. Ramandi, P. Craig, C. Gunawan, S. Wu, M. Manefield, A. Crosky, S. Saydam, *Eng. Failure Anal.* **2022**, *131*, 105884.

[27] A. Detman, D. Mielecki, A. Chojnacka, A. Salamon, M. K. Błaszczyk, A. Sikora, *Microb. Cell Fact.* **2019**, *18*, 1.
[28] C. Douglas Elliott, *Biomass, Chemicals from, 1st ed., Encyclopedia of Energy*, Pacific Northwest National Lab. (PNNL), Richland, WA **2004**.
[29] D. F. Drinan, S. Robin, T. M. Cogan, *Appl. Environ. Microbiol.* **1976**, *31*, 481.
[30] J. W. Leung, Y. L. Liu, T. Desta, E. Libby, J. F. Inciardi, K. Lam, *Gastrointestinal Endoscopy* **1998**, *48*, 250.
[31] J. Wimpenny, *Symposia-Society for General Microbiology*, Cambridge University Press, Cambridge **2000**, p. 1.

How to cite this article: A. Prithiraj, S. Tichapondwa, E. M. N. Chirwa, *Can. J. Chem. Eng.* **2024**, *102*(5), 1814. https://doi.org/10.1002/cjce.25154